On the decay of stratospheric pollutants: Diagnosing the longest-lived eigenmode

D. H. Ehhalt and F. Rohrer
Forschungszentrum Jülich, Institut II: Troposphäre, Jülich, Germany

S. Schauffler
National Center for Atmospheric Research, Boulder, Colorado, USA

M. Prather
Department of Earth System Science, University of California, Irvine, California, USA

Received 31 July 2003; revised 16 December 2003; accepted 19 January 2004; published 17 April 2004.

[1] On the basis of a one-dimensional (1-D) analysis the decay time of the lowest eigenmode, τ_1, for the stratospheric distribution of a conserved tracer is derived from measured vertical profiles of the mean age of stratospheric air. Two case studies (a and b) give $\tau_{1,a} = 3.8 \pm 0.8$ years and $\tau_{1,b} = 5.3 \pm 1.1$ years. These semiobservational times are considerably longer than most of the τ_1 derived from 2-D and 3-D models. At the same time they are shorter than the observational eigentime, $\tau_{1,HTO} = 7.7 \pm 2$ years, determined from the decay of the tritium (T) content in stratospheric water vapor, following the thermonuclear test explosions in the early 1960s. Part of the differences among the observational eigentimes can be explained by the assumptions that had to be made to extract $\tau_{1,HTO}$ from the trend in the T content of stratospheric water vapor (namely, the cosmogenic background of tritiated water vapor and the trend in stratospheric water vapor). This leads to a revised value $\tau_{1,HTO} = 6.3 \pm 0.9$ years for the time period 1975–1983. Allowing for a possible temporal trend in Γ and hence τ_1, the value for the current τ_1 decreases to 5.3 ± 1 years. *INDEX TERMS:* 0341 Atmospheric Composition and Structure: Middle atmosphere—constituent transport and chemistry (3334); 3334 Meteorology and Atmospheric Dynamics: Middle atmosphere dynamics (0341, 0342); 3362 Meteorology and Atmospheric Dynamics: Stratosphere/troposphere interactions; *KEYWORDS:* eigenfunctions of the vertical diffusion operator, residence time

Citation: Ehhalt, D. H., F. Rohrer, S. Schauffler, and M. Prather (2004), On the decay of stratospheric pollutants: Diagnosing the longest-lived eigenmode, *J. Geophys. Res.*, *109*, D08102, doi:10.1029/2003JD004029.

1. Introduction

[2] The rate of removal of pollutants from the stratosphere is a key factor in evaluating their respective environmental impacts. This rate relies to a large extent on the transport of the polluting trace constituents within and out of the stratosphere, which, in turn, is governed by the mean meridional Brewer-Dobson circulation [*Brewer*, 1949] superimposed on a quasi-horizontal eddy mixing [e.g., *Holton et al.*, 1995]. The circulation pumps tropospheric air into the stratosphere through the tropical tropopause, moves it upward and poleward in the tropics, poleward but downward at middle and high latitudes, and eventually returns it to the troposphere. The wave-driven mixing proceeds along isentropes in the midlatitudes, primarily in winter. Although the principal features of stratospheric transport are well understood, some of the details are not, and transport remains often poorly quantified in current chemical transport models [*Hall et al.*, 1999a, 1999b].

[3] It is therefore important to find diagnostics which allow the calibration of model transport against features of the real transport as evidenced in the measured temporal and spatial distributions of trace constituents. One such diagnostic is the eigentime of the lowest mode of the stratospheric transport equations for a conserved tracer. It has been shown for cyclostationary transport (e.g., constant or annually repeating wind fields) that the linearized chemistry-transport equations have a unique set of eigenvectors or modes, $F_n(\mathbf{x}, s)$ [*Prather*, 1996]. Each F_n describes the tracer abundance spatially ($\mathbf{x}$) and seasonally (s), and each decays exponentially with an *e*-fold time given by the inverse of its eigenvalue and called eigentime or τ_n here. Thus the spaciotemporal decay of a perturbation in the mixing ratio, $m(\mathbf{x}, t)$, of a stratospheric pollutant can be expressed as a unique combination of coefficients c_n and exponentially decaying modes F_n

$$m(\mathbf{x}, t) = \sum_{n=1}^{\infty} c_n \cdot F_n(\mathbf{x}, s) \cdot e^{-t/\tau_n} \quad (1)$$

0148-0227/04/2003JD004029

Equation (1) holds for any tracer, whether it is chemically reactive in the stratosphere or conserved. However, in the case of a conserved tracer with a strong sink in the lower troposphere or the Earth's surface, the τ_n only depend on transport. Moreover, because tropospheric transport is comparatively rapid, they virtually depend on stratospheric transport only. Since the τ_n decrease with n, the higher modes decay more readily. In the long term, only the lowest mode survives. Thus the eigentime of the lowest mode describes how fast the mixing ratio of a tracer will eventually decay everywhere in the stratosphere when acted upon by transport alone. The τ_1 describing a temporal response is conceptually and numerically different from the residence time, which defines the steady state turnover of a tracer [e.g., *Ehhalt et al.*, 2002]. It represents a unique diagnostic for stratospheric transport.

[4] A survey of model-calculated values for τ_1 was reported by *Hall et al.* [1999a]. For 3-D models τ_1 ranged from 1.4 years to 3.4 years with one outlier at 5.4 years. A recent analysis by *Ehhalt et al.* [2002] using tritium (T) injected from nuclear weapons tests provided the first observational determination of the eigentime of the longest mode for a conserved stratospheric tracer. It resulted in $\tau_{1,HTO} = 7.7 \pm 2$ years, considerably longer than all of the modeled τ_1.

[5] This large discrepancy makes it desirable to find other observational data from which τ_1 can be estimated. This paper investigates the possibility of estimating τ_1 from measured vertical profiles of the mean age of stratospheric air, $\Gamma(z)$. This is done in three steps. First, we show that in one dimension $\Gamma(z)$ is uniquely related to the profile of the vertical eddy diffusion coefficient, K(z). This allows to derive a globally averaged K(z) from the global average of measured $\Gamma(z)$, and thus to formulate a (globally averaged) one-dimensional (1-D) time-dependent vertical diffusion equation. This equation can be solved for τ_1, for instance, by using an eigenvalue analysis. Finally, to test the validity of the so derived τ_1 for a 3-D world, we apply this procedure to fields of Γ resulting from 3-D models and show that the τ_1 from the 1-D analysis of the model average $\Gamma(z)$ closely represent the τ_1 obtained directly from the 3-D models. The τ_1 obtained by the 1-D analysis from two examples (a and b) of observed $\Gamma(z)$ profiles are $\tau_{1,a} = 3.8$ years and $\tau_{1,b} = 5.3$ years and fall between the model obtained values and the value derived from the T content in stratospheric water vapor. A reexamination of the assumptions going into the derivation of $\tau_{1,HTO}$ leads to a downward revision of the original value of $\tau_{1,HTO} = 7.7 \pm 2$ years to 6.3 ± 0.9 years. A good part of the remaining difference to $\tau_{1,a}$ and $\tau_{1,b}$ can be possibly assigned to a change in $\Gamma(z)$ and hence in τ_1 with time.

2. Estimation of τ_1 From Measured Profiles of the Mean Age of Stratospheric Air

[6] The common definition for the age of stratospheric air is the time since last contact with the troposphere. Air parcels in the stratosphere consist of an inseparable mix of fluid elements with a distribution of ages, including some elements that are very old. The average over this distribution is the mean age Γ [*Hall and Plumb*, 1994], and, while the distribution of the age of air in a parcel is not an observable quantity, the mean age can be observationally derived from the stratospheric distributions of inert tracers with linearly increasing tropospheric abundance, such as CO_2 or SF_6 [*Schmidt and Khedim*, 1991; *Boering et al.*, 1996; *Harnisch et al.*, 1996]. This mean age generally increases with altitude and latitude, and an intercomparison of models and measurements [*Hall et al.*, 1999a] shows that modeled mean ages are typically younger than the measured ones by about a factor of 2 in the lower stratosphere. This discrepancy indicates that the stratospheric tracer transport in models is too fast, and it is consistent with the models' underestimate of τ_1. Here we use observed vertical profiles, $\Gamma(z)$, at midlatitudes to derive empirical values for τ_1. The derivation is based on the insight that in 1-D $\Gamma(z)$ is a unique function of the vertical profile of the eddy diffusion coefficient, K(z). Through inversion K(z) can therefore be obtained from $\Gamma(z)$. Once the globally averaged K(z) and hence the 1-D vertical eddy diffusion equation are known, τ_1 is readily calculated numerically [e.g., *Prather*, 1997; *Ehhalt et al.*, 2002].

2.1. Derivation of K(z) From $\Gamma(z)$

[7] Two distinct age profiles used for this purpose are shown in Figures 1a and 1b. They are adapted from Figures 2.12 and 2.10, respectively, of *Hall et al.* [1999a]. Figure 1a represents the average $\Gamma(z)$ in the extra tropics (poleward of 20° latitude) derived from in situ measurements of SF_6 and CO_2. These data are from balloon and aircraft flights, the latter made around 20 km altitude. They where first mapped against the simultaneously measured N_2O mixing ratios, which served as an surrogate altitude scale, and then converted to an equivalent pressure altitude scale by using the N_2O altitude profiles at midlatitudes from ATMOS and CLAES [*Hall et al.*, 1999a]. The Γ profiles of these two trace gases are in close agreement. They also closely resemble those derived in more recent work that includes more data and thus has greater global coverage extending from 70°S to the North Pole [*Andrews et al.*, 2001]. This work includes tropical data. Thus we view $\Gamma_a(z)$ to also represent the global average. A fit of a third-order polynomial to the weighted average of the two profiles in Figure 1a yields

$$\Gamma_a(z) = -0.17042 + 0.49054 \cdot \Delta z - 0.013386 \cdot \Delta z^2 + 0.00008838 \cdot \Delta z^3 \quad (2)$$

where Γ is in years and Δz is the height above the tropopause, assumed here to be at 12 km: $\Delta z = z - 12$.

[8] The second age profile (Figure 1b) was included, because the K(z) profile eventually derived from it is similar in form and absolute value to the K(z) profiles used in the 1-D modeling of stratospheric chemistry some years back (see Figure 2). It is based on the CO_2 and SF_6 measurements of the OMS balloon flight 21 September 1996 at 34°N latitude. The scale of $\Gamma(z)$, however, is shifted by about 1 year with respect to that given by *Hall et al.* [1999a] to produce an age of zero at the tropopause. These data are fitted by a fourth-order polynomial, because this Γ profile displays a higher order of vertical structure with an inflection point at 20 km altitude.

$$\Gamma_b(z) = 0.0425 - 0.20433 \cdot \Delta z + 0.147045 \cdot \Delta z^2 - 0.010228 \cdot \Delta z^3 + 0.00020977 \cdot \Delta z^4 \quad (3)$$

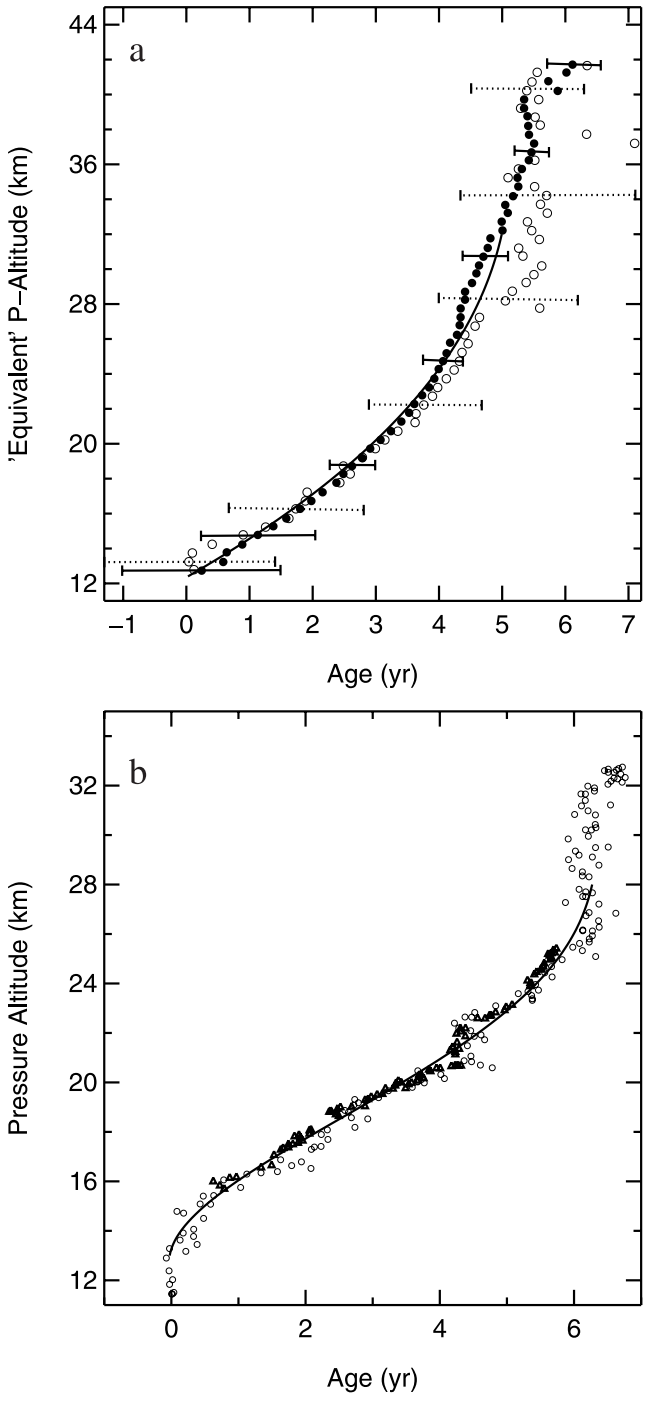

Figure 1. Vertical profiles of the mean age (years) as a function of pressure altitude (z), adapted from *Hall et al.* [1999a]. (a) Mean age averaged over the extra tropics (poleward of 20° latitude). Open circles represent in situ measurements of SF_6; full circles represent in situ measurements of CO_2, both from aircraft and balloons in a number of campaigns (SPADE, ASHOE-MAESA, STRAT, POLARIS, and OMS). Bars indicate the 2-sigma standard deviations of the averages. (b) Mean age from the OMS balloon flight on 21 September 1996 at 34°N latitude. Triangles represent in situ measurements of CO_2; circles represent in situ measurements of SF_6. The scale of the abscissa has been shifted by +1 year to match the data at 12 km altitude with an age of zero.

The fitted age profiles $\Gamma_a(z)$ and $\Gamma_b(z)$ are valid in the altitude ranges of 12–32 km and 13–28 km, respectively.

[9] Both age profiles are subject to uncertainties. On the basis of the observation that the empirical uncertainty of $\Gamma(z)$ given in Figure 1a averages 1 year, that the $\Gamma(z)$ increase monotonically with altitude, and that $\Gamma(z)$ must be zero at the tropopause, we assume a common error factor of 1.2 at all altitudes for $\Gamma_a(z)$ and $\Gamma_b(z)$. A general discussion of the uncertainties involved in deriving $\Gamma(z)$ from CO_2 measurements is given by *Andrews et al.* [2001].

[10] To convert $\Gamma(z)$ into an effective 1-D vertical profile of the eddy diffusion coefficient, K(z), we make use of relation (4) which is derived in Appendix A.

$$\Gamma(z) = H \cdot \int_{12km}^{z} \frac{dz'}{K(z')} \tag{4}$$

where z is the altitude, the tropopause is at 12 km, and $H \approx 7$ km is the scale height in the stratosphere.

[11] Differentiating equation (4) and solving for K(z), we obtain

$$K(z) = H \Big/ \frac{d\Gamma(z)}{dz} \tag{5}$$

Inserting $\Gamma_a(z)$ and $\Gamma_b(z)$ into equation (5) and converting to units of $m^2\ s^{-1}$ yields

$$K_a(z) = H\left(15.452 - 0.8433 \cdot \Delta z + 0.008352 \cdot \Delta z^2\right)^{-1} \tag{6}$$

$$K_b(z) = H(-6.4364 + 9.2638 \cdot \Delta z - 0.9665 \cdot \Delta z^2 + 0.02646 \cdot \Delta z^3)^{-1} \tag{7}$$

where H and Δz are given in units of km and K is given in units of $(m^2\ s^{-1})$.

[12] The two K profiles, $K_a(z)$ and $K_b(z)$ are shown in Figure 2 along with some K profiles used in or recommended for 1-D modeling of stratospheric chemistry in the earlier literature. Their display is limited to the altitude range between 14.5 km and 29.5 km, because some of the earlier profiles start at 15 km and $K_b(z)$ is only applicable up to 28 km. The profiles marked by W, Di, and Da were derived from fits of 1-D modeled profiles of CH_4, CH_4 and N_2O, and O_3, respectively, to the corresponding measured trace gas profiles obtained at northern midlatitudes, mostly at 30°N [*Wofsy and McElroy*, 1973; *National Research Council Panel on Atmospheric Chemistry*, 1976; *Panel on Stratospheric Chemistry and Transport*, 1979]. The profile marked by H was derived by *Holton* [1986] based on a meridional average over an approximate 2-D transport model of the stratosphere. Ch indicates a profile used by *Chang* [1974].

[13] On the whole, the two profiles $K_a(z)$ and $K_b(z)$ obtained from the age profiles in Figure 1 fall well within the range spanned by the earlier profiles. It is interesting to note, however, that $K_a(z)$, which is based on a global, i.e., two-dimensional altitude-by-latitude average, shows a monotonic increase with altitude similar to profile H derived

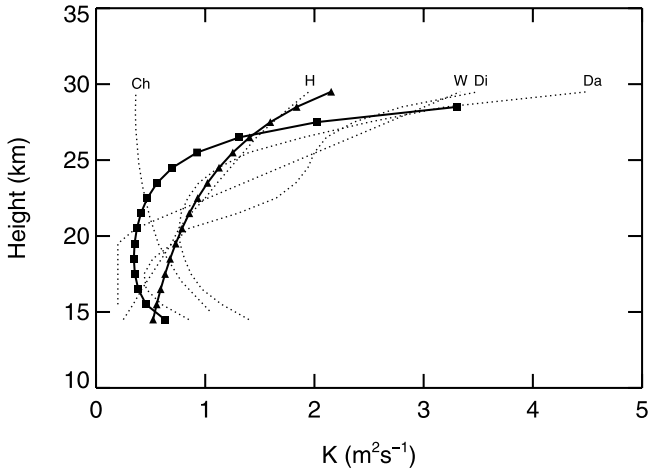

Figure 2. Vertical profiles of the 1-D vertical eddy diffusion coefficient K (m^2 s^{-1}) as a function of altitude from 14.5 to 29.5 km altitude. The bold curves are derived from the mean age profiles given in Figure 1; triangles represent the profile K_a; squares represent the profile K_b. For comparison, K profiles used or recommended for 1-D modeling of stratospheric chemistry are indicated by the thin lines (see text for details).

from a 2-D analysis, whereas $K_b(z)$ based on a Γ profile obtained for 34°N latitude displays a C-shaped profile similar to profiles Da, Di, and W derived from midlatitude vertical tracer profiles.

[14] For the determination of the respective eigentimes the profiles $K_a(z)$ and $K_b(z)$ need to be extended to higher altitudes. To capture the possible range we choose three different extensions:

$$\begin{aligned}
&32\text{ km} > z \geq 12\text{ km}: K_{a,1}(z) = K_{a,2}(z) = K_{a,3}(z) = K_a(z)\\
&z \geq 32\text{ km}: K_{a,1}(z) = 3.6\text{ m}^2\text{s}^{-1}\\
&\qquad K_{a,2}(z) = 3.6 \cdot e^{((z-32)/2H)}\text{ m}^2\text{s}^{-1}\\
&\qquad K_{a,3}(z) = 3.6 \cdot e^{((z-32)/H)}\text{ m}^2\text{s}^{-1}\\
&28\text{ km} > z \geq 13\text{ km}: K_{b,1}(z) = K_{b,2}(z) = K_{b,3}(z) = Kb(z)\\
&z > 28\text{ km}: K_{b,1}(z) = 2.6\text{ m}^2\text{s}^{-1}\\
&\qquad K_{b,2}(z) = 2.6 \cdot e^{((z-28)/2H)}\text{ m}^2\text{s}^{-1}\\
&\qquad K_{b,3}(z) = 2.6 \cdot e^{((z-28)/H)}\text{ m}^2\text{s}^{-1}
\end{aligned} \tag{8}$$

In both cases the most probable upper altitude extension is given by the altitude dependence $e^{z/2H}$ [cf. *Lindzen*, 1968]. The two others serve to estimate the uncertainty introduced by the need to extend $K_a(z)$ and $K_b(z)$ to higher altitudes.

2.2. Determination of τ_1

[15] The eigentime of the lowest mode can be determined in two ways. One is, to approximate the 1-D diffusion equation (A2) by finite differences and solve the matrix numerically for all eigenvalues and eigenvectors [e.g., *Prather*, 1997]. We preferred a second method, because we were also interested in the age spectrum. It relies on the fact that τ_1 also describes the decay of the age spectrum of stratospheric air toward higher ages [*Hall et al.*, 1999a]. The age spectra for different altitudes can be obtained by numerically solving the time-dependent transport equation for a pulsed tracer injection at the tropopause. The spectrum at any location in the stratosphere is given by the temporal evolution of the tracer mixing ratio. The τ_1 derived from the *e*-fold of the tail of this spectrum is identical for all altitudes as expected [*Prather*, 1996]. Solving equation (A2) given in Appendix A for the stratospheric K(z) profiles specified in section 2.1, a tropospheric eddy diffusion coefficient, K = 10 m^2 s^{-1}, and a tropopause at 12 km altitude, yields the τ_1 listed in Table 1. The height resolution is 1 km, and the boundary conditions are m = 0 at the ground and $\partial m/\partial z = 0$ at 82 km altitude. The values for τ_1 depend slightly on the vertical resolution and the height of the upper boundary. This dependence is less than 1% for the K(z) used here, as long as the resolution is better then 1 km and the upper boundary is above 82 km.

[16] As indicated previously, we consider the $a \cdot e^{z/2H}$ as the most likely extension of K(z) to higher altitudes. Accordingly $\tau_{1,a}$ = 3.83 years and $\tau_{1,b}$ = 5.27 years are the most likely eigentimes for $K_a(z)$ and $K_b(z)$. We also note that the precise form of the extension of K(z) to higher altitudes does not add much variance to the respective values of τ_1. To be conservative, we assume that the error contributed from the possibility of different extensions with altitude is given by the larger of the two deviations. Most of the error in the τ_1 comes from the error in the K(z) as derived from the $\Gamma(z)$. The error factor of 1.2 assumed for the $\Gamma(z)$ at all altitudes propagates linearly into the error of τ_1, because that factor propagates linearly to K(z) and τ_1 is proportional to $K(z)^{-1}$. Thus the errors of the τ_1 are roughly ±20% including the uncertainty in the extrapolation of K(z) as an independent error.

$$\tau_{1,a} = 3.8 \pm 0.8\text{ years}$$

$$\tau_{1,b} = 5.3 \pm 1.1\text{ years}$$

2.3. Applicability of $\tau_{1,a}$ and $\tau_{1,b}$ in Three Dimensions

[17] The present derivation of τ_1 relies on a 1-D model, which obviously provides only a crude approximation of the real 3-D transport in the stratosphere, raising the question whether the so derived τ_1 is a useful approximation to the real τ_1. Moreover, the use of globally or regionally averaged

Table 1. Eigentimes of the Lowest Mode, τ_1, in Years for the Various Profiles of the Stratospheric Vertical Eddy Diffusion Coefficient, K(z), Derived in Section 2

K(z)	τ_1
$K_{a,1}$	3.92
$K_{a,2}$	3.83
$K_{a,3}$	3.79
$K_{b,1}$	5.59
$K_{b,2}$	5.27
$K_{b,3}$	5.25

Table 2. Comparison of $\tau_{1,3D}$ Obtained Directly From 3-D Model Calculations [*Hall et al.*, 1999a] With $\tau_{1,Ci}$ Derived From the 1-D Γ Profiles Using Four Different Averaging Procedures (C1, C2, C3, and C4) to Obtain a Global Mean From Modeled Γ Distributions

Model	$\tau_{1,3D}$, years	$\tau_{1,C1}$, years	$\tau_{1,C2}$, years	$\tau_{1,C3}$, years	$\tau_{1,C4}$, years
GISS	2.19	2.20	-	2.31	
GMI DAO	1.44	1.24	1.20	1.24	
NCAR	2.89	2.87	2.57	2.70	
GSFC 3D	1.56	1.26	-	1.25	
MONASH 1	5.41	3.40	3.38	3.51	
MONASH 2	2.89	2.70	2.51	2.53	
UCI 23	3.14	3.39	3.30	3.63	
UIUC 3D	1.74	1.17	0.98	1.11	
UNIVAC 3D	2.36	2.31	2.16	2.37	
UCI-1977	4.56		4.92		4.9
UCI-1978	4.75				

vertical profiles of measured Γ may introduce a bias. Thus we have to test whether $\tau_{1,a}$ and $\tau_{1,b}$ are representative of a realistic stratosphere with three-dimensional transport. To a certain extent such a test is feasible based on the comparison of several 3-D models presented by *Hall et al.* [1999a]. In addition to τ_1 for the various models, that paper also presents zonally and annually averaged distributions of Γ (and N_2O) calculated by nine (seven) of the models. From these distributions a globally averaged 1-D vertical profile of Γ can be calculated, and τ_1 can be derived from the method described above. For that purpose, Figures 2.19 and 2.29 from *Hall et al.* [1999a] were digitized to yield Γ and N_2O values every 1 km altitude and 5° latitude. Using different averaging procedures, we can investigate how much these influence τ_1 and how much the so derived τ_1 deviate from that directly calculated by the models. Table 2 presents three cases of averaging for the nine published model results plus another case for the UCI CTM rerun specifically for this study:

[18] 1. For case 1, average Γ over latitudes at constant altitudes.

[19] 2. For case 2, average Γ over latitudes at constant N_2O abundances to derive a global mean $\Gamma(N_2O)$ which is converted to $\Gamma(z)$ using the mean N_2O profile at 30°N.

[20] 3. For case 3, use the vertical $\Gamma(z)$ profile at 35°N latitude as proxy for the global average.

[21] Cases 1 and 2 approximate the averaging procedure used for the observational $\Gamma_a(z)$, and case 3 approximates the observational $\Gamma_b(z)$, which was obtained at 34°N latitude on 21 September 1996. Interestingly, the average Γ profile resulting from cases 1 and 2 have all the functional form of Γ_b. For a given model they agree, mostly within 10%. The differences of Γ between models can be large. The values for Γ (30 km) at 30°N in Figure 3 provide an indication of the range in Γ between the models, the more so since they closely agree with the values at 30 km of the globally averaged Γ profiles.

[22] To better simulate $\Gamma_a(z)$, we also present case 4, which is based on new calculations from the UCI CTM with meteorological fields (4° latitude × 5° longitude × 23 layers resolution) from a more recent version of the GISS stratospheric circulation model [*Rind et al.*, 1999] and monthly 3-D snapshots of Γ being saved.

[23] 4. For case 4, shift the tropopause (defined as Γ = 0.5 years) of the local, monthly Γ profiles to a common altitude of 14 km before calculating the global annual average.

[24] Like $\Gamma_a(z)$, case 4 avoids smearing of the mean vertical gradient in Γ due to longitudinal and seasonal variations in the tropopause.

[25] As to be expected from the wide range of stratospheric transport represented by the models, the $\tau_{1,3D}$ vary widely. Nevertheless, there are no obvious biases between the different averaging procedures. For seven of the nine models in the *Hall et al.* [1999a] study, the $\tau_{1,Ci}$ underestimate $\tau_{1,3D}$ by about 1% to 40%. The exceptions are the GISS and UCI 23 models as well as the new UCI-1997 results, all of which use GISS meteorological fields, and whose $\tau_{1,Ci}$ overestimate $\tau_{1,3D}$. On average the $\tau_{1,Ci}$ agree to within 10% with the respective $\tau_{1,3D}$ excepting MONASH 1. Together this suggests that the semiobservational eigentimes $\tau_{1,a}$ and $\tau_{1,b}$ derived from observed Γ are equally valid estimates of τ_1 but that they possibly underpredict τ_1 by about 10%.

[26] Year-to-year variations of τ_1 are investigated with new UCI CTM calculations using meteorological fields from two consecutive years of the GISS-II' middle atmosphere model, labeled 1977 and 1978. The resulting 4% difference in $\tau_{1,3D}$ is shown in Table 2. Such year-to-year variability is similar in magnitude to that diagnosed with the GISS model for N_2O and $CFCl_3$ lifetimes [*Wong et al.*, 1999], and we can expect a specific year, as reported by *Hall et al.* [1999a], to be representative within about 4%.

2.4. A Simple Empirical Relationship Between τ_1 and $\Gamma(z)$

[27] The derivation of τ_1 from $\Gamma(z)$ shows that both are related, a fact already been pointed out by *Hall et al.*

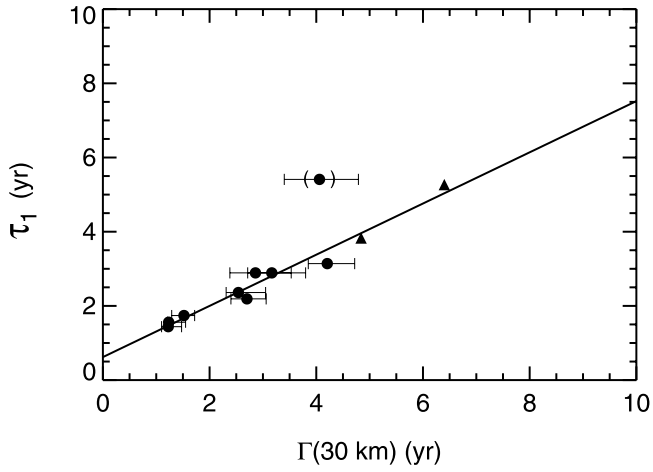

Figure 3. Relation of τ_1 (years) and the mean age Γ (years) at 30 km altitude. The triangles represent the semiobservational values, corresponding to the mean age profiles Γ_a and Γ_b in Figure 1. The circles represent the modeled $\tau_{1,3D}$ and Γ (30 km) at 30°N latitude [*Hall et al.*, 1999a, Figure 2.19] (see also Table 2). The MONASH-1 results are shown in parentheses. The horizontal whiskers indicate the range of Γ(30 km) from 20°N to 50°N. The straight line is a linear regression fit to the model and observational data without MONASH-1 (see text).

[1999a, Figure 2.26]. To find a simple scaling (as opposed to the integrative relationship established above), we plot τ_1 versus Γ(30 km) for Γ at northern midlatitudes where most of the measurements are located (Figure 3). The altitude of 30 km is chosen because it fully utilizes the vertical extent of the observational Γ, and K(z) above 30 km has little impact on τ_1. The semiobservational $\tau_{1,a/b}$ are plotted versus $\Gamma_{a/b}$(30 km) as triangles. The modeled $\tau_{1,3D}$ are plotted versus Γ(30 km) at 30°N as circles, with whiskers denoting the range in Γ(30 km) from 20°N to 50°N. Figure 3 demonstrates that, apart from MONASH 1, the 3-D models and the observational data follow a common and virtually linear relation:

$$\tau_1 = (0.69 \pm 0.05)\Gamma(30\text{km}) + (0.62 \pm 0.22) \qquad (9)$$

While the ($\tau_{1,a/b}$, $\Gamma_{a/b}$) relationship is by derivation tightly coupled, the modeled $\tau_{1,3D}$ were calculated from the decay of a stratospheric tracer and thus are not directly related to the modeled Γ. Therefore this linear relationship should be relatively robust. It provides another, convenient way to estimate τ_1 from Γ observed at northern midlatitudes and could be refined as new measurements better define the global distribution of Γ.

3. Reconciling the Different Observationally Derived τ_1

[28] While the semiobservational eigentimes $\tau_{1,a} = 3.8 \pm 0.8$ years and $\tau_{1,b} = 5.3 \pm 1.1$ years derived here are larger than most of the modeled $\tau_{1,3D}$, they are also smaller than the observational $\tau_{1,HTO} = 7.7 \pm 2$ years derived from the analysis of the decay of the T content in stratospheric water vapor [*Ehhalt et al.*, 2002]. At least for $\tau_{1,a}$ the difference relative to $\tau_{1,HTO}$ is statistically significant. There are a number of factors that could contribute to this difference, and we first reexamine the derivation of $\tau_{1,HTO}$.

3.1. Correction of $\tau_{1,HTO}$

[29] The derivation of $\tau_{1,HTO}$ was based on measurements of the T/H ratio in stratospheric water vapor between 1975 and 1983 which showed an exponential decay mainly resulting from the large HTO injections from thermonuclear explosions in the early 1960s. To extract from this measured decay the contribution of the HTO loss due to transport into the troposphere, characterized by $\tau_{1,HTO}$, other processes that impact the T/H ratio had to be quantified. Some of these were poorly known and had to be estimated, e.g., the natural, cosmogenic production of HTO; injections of HTO into the stratosphere due to thermonuclear explosions between 1975 and 1983; and any trend in stratospheric H_2O. In fact, most of the uncertainty in $\tau_{1,HTO}$ resulted from the uncertainties in these estimates [*Ehhalt et al.*, 2002]. In the following we reexamine the assumptions entering these estimates to see whether they could have contributed to the difference between $\tau_{1,HTO}$ and $\tau_{1,a/b}$.

3.1.1. Natural Tritium Levels

[30] For simplicity, *Ehhalt et al.* [2002] assumed that the HTO background, B, due to cosmogenic production was negligible. This assumption was based on a fit of the expression $A \cdot e^{-t/\tau} + B$ to the measured decrease in the T/H ratios which resulted in a $B = -(1.12 \pm 1.86) \cdot 10^6$ TU, a value not significantly different from zero (1 tritium unit, TU, corresponds to a T/H ratio of 10^{-18}). There is, however, another way of fitting the decrease, namely, by fitting log(T/H) with the expression $\log(A \cdot e^{-t/\tau} + B)$. In this case we obtain a more plausible value, $B = 0.22 \cdot 10^6$ TU. It lies nearly midway between 0 and $0.5 \cdot 10^6$ TU which represents the stratospheric average background due to cosmogenic HTO and serves as an upper limit for that background at 30°N latitude [*Ehhalt et al.*, 2002]. Choosing $B = +0.25 \pm 0.25 \cdot 10^6$ TU for the cosmogenic background and fitting $\log(A \cdot e^{-t/\tau} + B)$ to the log(T/H) data, one obtains $\tau = 4.88 \pm 0.24$ years for the *e*-fold time of the temporal decrease in the T/H ratio. This correction is only a small adjustment to the original $\tau = 5.12 \pm 0.7$ years derived for $B = 0$, but it removes a systematic error.

3.1.2. Subsequent Thermonuclear Injections

[31] The atmospheric thermonuclear test in October 1976 over Lop Nor, China, 41°N latitude, injected HTO into the lower stratosphere [*Mason et al.*, 1982]. The impact of that injection was clearly visible in the T/H ratio of the water vapor sampled at the two lowest altitudes of the balloon flight over Yorkton, Canada, on 14 March 1977, but not in the altitudes above [*Ehhalt et al.*, 2002, Figure 4]. Some of that injected HTO could also have influenced the subsequent flight on 30 April 1978 over Fairbanks, Alaska. *Ehhalt et al.* [2002] assumed that removal of the T/H measurements at the two lowest altitudes of the flight on 14 August 1977 from the data set would fully remove the impact of this injection. If this assumption were incorrect, then the average T/H ratio from the subsequent flight might be too high resulting in a slower apparent decay rate. To test this possibility, we also removed the entire flight over Fairbanks from the data set and fitted the remaining data by $\log(A \cdot e^{-t/\tau} + B)$, with $B = 0$, $0.25 \cdot 10^6$ and $0.5 \cdot 10^6$ TU. The resulting τ are virtually the same as those for the full set of profiles. This corroborates the earlier assumption and there is no need for an adjustment.

3.1.3. Trends in Stratospheric H_2O

[32] The most critical assumption concerned the trend of stratospheric H_2O. Without independent measurements of the H_2O mixing ratio for the balloon flights near 32°N between 1975 and 1983, *Ehhalt et al.* [2002] adopted the long-term globally averaged trend of H_2O of 1% yr^{-1} recommended by *Stratospheric Processes and their Role in Climate* (*SPARC*) [2000]. It was assigned an error of ± 2% yr^{-1} to account for the possibility that regionally and temporarily the trend in H_2O could have been negative. Such a temporary deviation from the mean trend lasting a few years is not uncommon, as *Rosenlof et al.* [2001] have shown for the CMDL data over Boulder.

[33] Rather than adopting the long-term global trend, here we examine what stratospheric H_2O data are available around the time period and latitude of the HTO measurements. Figure 4, adapted from *SPARC* [2000], summarizes the water vapor record for northern midlatitudes and the time period 1965–1990. It applies to an altitude of about 26 km, the center of the altitude range sampled by the HTO measurements. A similar figure exists for 19 km altitude (60–70 hPa) whose data exhibit the same behavior [*SPARC*, 2000; *Rosenlof et al.*, 2001]. First of all, Figure 4 demonstrates the scarcity of the H_2O data during 1975–1983. Only three instruments contributed to the H_2O record of that

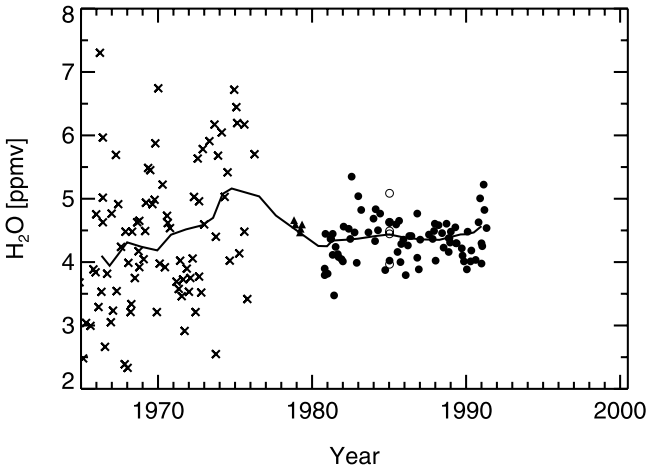

Figure 4. Measurements of stratospheric water vapor (ppm) at 21 hPa pressure (~26 km altitude) and 30°–50°N latitude from 1965 to 1990 (adapted from *SPARC* [2000]). Shown are the in situ, balloon-borne frost point hygrometer measurements by NRL (crosses), those by CMDL (solid circles), and the satellite infrared spectroscopic measurements from LIMS (triangles) and ATMOS (open circles). The thin curve represents the 5-year running average over these data.

period: The frost point hygrometer of the Naval Research Laboratory (NRL) (crosses), its improved version of the Climate Monitoring and Diagnostics Laboratory (CMDL) (solid circles) and the satellite-borne infrared radiometer, LIMS (triangles). The NRL data were taken over Washington, D. C., the CMDL data were taken over Boulder, Colorado, and the LIMS data were longitudinally distributed. Moreover, the observation intervals of these three instruments are separated by rather large time gaps, and the instruments were not intercalibrated. In addition, the NRL data exhibit a good deal of scatter, probably attributable to experimental difficulties. Thus the H_2O record from 1975 to 1983 is rather nonuniform and uncertain. Yet the evidence, however weak, points to a decrease in stratospheric H_2O at northern midlatitudes for the time period of the HTO measurements. This is emphasized by the 5-year running average (solid line) over these data, which shows a decrease of up to 3% yr^{-1} over most of that time interval.

[34] To allow for this possibility of a negative trend, we maintain the long-term global trend of +1% yr^{-1} as the upper limit and adopt −3% yr^{-1} from Figure 4 as the lower limit for the temporary and regional trend in stratospheric H_2O during the HTO measurements. We further choose the center of that interval, namely, −1% yr^{-1}, as the most likely value with the upper/lower limits as the 1-sigma range of the H_2O trend from 1975 to 1983 at 30°N.

[35] The $\tau_{1,HTO}$ resulting from this new estimate is readily calculated from

$$\tau_{1,HTO}^{-1} = \tau^{-1} - \tau_R^{-1} + \tau_{H_2O}^{-1} \quad (10)$$

where τ_R = 17.8 years is the radioactive decay time of tritium, $\tau = 4.88 \pm 0.24$ years is the observed decay time of the T/H ratio in stratospheric water vapor, and the inverse decay time $\tau_{H2O}^{-1} = (0.01 \pm 0.02)$ yr^{-1} characterizes the (negative) trend just estimated. With these values $\tau_{1,HTO} = 6.3 \pm 0.9$ years, still much larger than the $\tau_{1,3D}$ from the models. The difference to the previous value of 7.7 ± 2 years is mainly due to the different assumption about the trend in stratospheric water vapor. The difference in the respective errors of $\tau_{1,HTO}$ is due to the fact that the earlier estimate assumed a HTO background of 0 but allowed a large symmetric error to cover the maximum background. This error therefore amounted to $\pm 0.5 \times 10^6$ TU, twice as large as that adopted here [see *Ehhalt et al.*, 2002].

3.2. Temporal Change in τ_1

[36] Although still larger, the revised $\tau_{1,HTO}$ is in reasonable agreement with $\tau_{1,b}$. It remains significantly different, however, from $\tau_{1,a}$ derived from the globally averaged age profile. Another, geophysical, reason for the disagreement may be that τ_1 has changed with time; $\tau_{1,HTO}$ is determined for the period 1975–1983, whereas the Γ are based on data obtained after 1990. Thus we consider the temporal evolution of $\Gamma(z)$, which evolves similarly to τ_1. *Andrews et al.* [2001] summarize the determinations of Γ in the middle stratosphere (circa 25–30 km) at northern midlatitudes based on measurements of CO_2 over the last 25 years by various authors. From their Figure 10, *Andrews et al.* [2001] conclude that over this period Γ remained within ± 1 year of its current mean value of 4.5 years. This is certainly correct. A closer inspection reveals, however, that the older measurements from 1975 to 1983 tend to fall above the average age by $+0.46 \pm 0.25$ year, whereas the measurements since 1990 fall below by -0.40 ± 0.18 year, even if the outlier of −3 years below by *Harnisch et al.* [1998] is disregarded. The errors given represent the statistical errors of the mean. That means that Γ of the earlier period differs from the newer one by +0.86 year or about 20%. Barring systematic errors in the measured Γ, for instance, from a drift in the calibration of the CO_2 measurements, this also means that $\tau_{1,HTO}$ = 6.3 years derived for the earlier period could be about 20%, or about 1 year, longer than any τ_1 derived from data after 1990. A decrease in τ_1 with time is not implausible. 3-D model calculations predict an increase in the stratospheric meridional circulation induced by the climate changes from the increasing levels of greenhouse gases [*Rind et al.*, 1998; *Butchart and Scaife*, 2001]. These predictions refer to the future and result in smaller rates of change, 3–5% $decade^{-1}$, than that indicated here, which amounts to about 12% $decade^{-1}$. Nevertheless, they underline the possibility of a long-term decrease in τ_1, which provides another step to reconcile the τ_1 derived from mean age profiles in the 1990s with that derived from the HTO profiles in the late 1970s. Adopting a past change in Γ of 20%, the $\tau_{1,HTO}$ for the time period 1973–1983 transforms into $\tau_{1,HTOc} = 5.3 \pm 1$ years in today's stratosphere, where the error given is based on the error in $\tau_{1,HTO}$ and the errors in the temporal averages of measured Γ from above. Any systematic bias in the determination of Γ from CO_2 profiles would tend to increase this error. The value for $\tau_{1,HTOc}$ is in good agreement with $\tau_{1,a}$ and $\tau_{1,b}$.

4. Summary and Conclusions

[37] We have shown that it is possible to derive a semi-observational τ_1 from the observed global average profile of

the mean age of stratospheric air $\Gamma(z)$. The values for two different $\Gamma(z)$ were $\tau_{1,a} = 3.8 \pm 0.8$ years and $\tau_{1,b} = 5.3 \pm 1.1$ years. Using 3-D models, we demonstrate that deriving these τ_1 from a 1-D diffusion analysis should apply also to the realistic three-dimensional stratospheric circulation. Reexamination and adjustment of the assumptions going into an earlier observational $\tau_{1,HTO} = 7.7 \pm 2$ years leads to a lower value, $\tau_{1,HTO} = 6.3 \pm 0.9$ years, for the time period 1975–1983. The remaining difference with respect to $\tau_{1,a}$ and $\tau_{1,b}$ can possibly be explained by a temporal trend in Γ and τ_1, which might be induced by global warming. Our estimate of the current $\tau_{1,HTOc}$ is 5.3 ± 1 years. This updated $\tau_{1,HTOc}$ remains significantly larger than the $\tau_{1,3D}$ from most current stratospheric models. The large observational τ_1 indicate that stratospheric transport is slower and that perturbations to total chlorine decay more slowly than predicted by current models, a conclusion which applies in particular to the persistence of the Antarctic ozone hole.

Appendix A: One-Dimensional Relationship Between Vertical Profiles of Mean Age of Air and Vertical Eddy Diffusion in the Stratosphere

[38] The age of stratospheric air is usually derived from vertical profiles of a conservative tracer that originates in the troposphere and whose source strength increases with time. The age of stratospheric air at altitude z, $\Gamma(z)$, is then defined as the time lag after which a given abundance at the tropopause reaches that altitude.

[39] *Hall and Plumb* [1994] showed that this definition is unique in the case of a tracer with a linear increase and in the long-term limit. In this case the vertical profile of age in the stratosphere, i.e., $\Gamma(z)$, becomes stationary in time, and the mixing ratio of the tracer at the tropopause, m(0, t) varies with the time, t, as

$$m(0,t) = m_o + s(t - t_o) \tag{A1}$$

where we have assigned the value z = 0 to the tropopause altitude and m $(0, t_o) = m_o$.

[40] From these two conditions we can construct a solution of the one-dimensional eddy diffusion equation:

$$\rho \cdot \frac{\partial m(z,t)}{\partial t} = \frac{\partial}{\partial z} \cdot \rho \cdot K(z) \cdot \frac{\partial m(z,t)}{\partial z} \tag{A2}$$

for the boundary conditions (A1). Here $\rho = \rho_o \cdot e^{-z/H}$ is the number density of air, and K(z) is the vertical eddy diffusion coefficient, which is allowed to vary with altitude.

[41] From the definition of $\Gamma(z)$ follows

$$m(z,t) - m(0, t - \Gamma(z)) = 0 \tag{A3a}$$

or inserting equation (A1),

$$m(z,t) = m_0 + s \cdot (t - \Gamma(z) - t_0) \tag{A3b}$$

which is the desired solution, provided $\Gamma(z)$ can be guessed. Clearly, the expression for $\Gamma(z)$ has to have a form such that equation (A3b) satisfies the differential equation (A2).

[42] For $K(z) = K_o = \text{const}$, *Hall and Plumb* [1994] derived

$$\Gamma(z) = \frac{H \cdot z}{K_0}. \tag{A4}$$

Generalizing this expression, we propose that

$$\Gamma(z) = H \cdot \int_0^z \frac{dz'}{K(z')} \tag{A5}$$

for a height-dependent K(z).

[43] Inserting equation (A5) into equation (A3b) indeed solves differential equation (A2), which proves that equation (A5) represents the correct age profile for a linearly increasing tracer in a 1-D approach.

References

Andrews, A. E., et al. (2001), Mean ages of stratospheric air derived from in situ observations of CO_2, CH_4, and N_2O, *J. Geophys. Res.*, *106*, 32,295–32,314.

Boering, K. A., S. C. Wofsy, B. C. Daube, H. R. Schneider, M. Loewenstein, and J. R. Podolske (1996), Stratospheric mean ages and transport rates from observations of carbon dioxide and nitrous oxide, *Science*, *274*(5291), 1340–1343.

Brewer, A. W. (1949), Evidence for a world circulation provided by the measurements of helium and water vapour distribution in the stratosphere, *Q. J. R. Meteorol. Soc.*, *75*, 351–363.

Butchart, N., and A. A. Scaife (2001), Removal of chlorofluorocarbons by increased mass exchange between the stratosphere and troposphere in a changing climate, *Nature*, *410*, 799–802.

Chang, J. S. (1974), Simulations, perturbations and interpretations, in *Proceedings of the Third Conference on the Climatic Impact Assessment Program*, *Rep. DOT-TSC-OST-74-15*, pp. 330–431, U.S. Dep. of Transp., Washington, D. C.

Ehhalt, D. H., F. Rohrer, S. Schauffler, and W. Pollock (2002), Tritiated water vapor in the stratosphere: Vertical profiles and residence time, *J. Geophys., Res.*, *107*(D24), 4757, doi:10.1029/2001JD001343.

Hall, T. M., and R. A. Plumb (1994), Age as a diagnostic of stratospheric transport, *J. Geophys. Res.*, *99*, 1059–1070.

Hall, T. H., D. J. Wuebbles, K. A. Boering, R. S. Eckman, J. Lerner, R. A. Plumb, D. H. Rind, C. P. Rinsland, D. W. Waugh, and C.-F. Wei (1999a), Transport experiments, in *Models and Measurements Intercomparison II*, edited by J. H. Park et al., *Rep. NASA/TM-1999-20,9554*, chap. 2, pp. 110–189, NASA, Hampton, Va.

Hall, T. M., D. W. Waugh, K. A. Boering, and R. A. Plumb (1999b), Evaluation of transport in stratospheric models, *J. Geophys. Res.*, *104*, 18,815–18,839.

Harnisch, J., R. Borchers, P. Fabian, and M. Maiss (1996), Tropospheric trends for CF_4 and C_2F_6 since 1982 derived from SF_6 dated stratospheric air, *Geophys. Res. Lett.*, *23*, 1099–1102.

Harnisch, J. W., W. Bischof, R. Borchert, P. Fabian, and M. Maiss (1998), A stratospheric excess CO_2-due to tropical deep convection, *Geophys. Res. Lett.*, *25*, 63–66.

Holton, J. R. (1986), A dynamically based transport parameterization for one-dimensional photochemical models of the stratosphere, *J. Geophys. Res.*, *91*, 2681–2686.

Holton, J. R., P. H. Haybes, M. E. McIntyre, A. R. Douglass, R. B. Rood, and L. Pfister (1995), Stratosphere-troposphere exchange, *Rev. Geophys.*, *33*(4), 403–439.

Lindzen, R. S. (1968), The application of classical atmospheric tidal theory, *Proc. R. Soc. London A*, *303*, 299–316.

Mason, A. S., G. Hut, and K. Telegadas (1982), Stratospheric HTO and ^{95}Zr residence times, *Tellus*, *39*, 369–375.

National Research Council Panel on Atmospheric Chemistry (1976), *Halocarbons: Effects on Stratospheric Ozone*, Natl. Acad. of Sci., Washington, D. C.

Panel on Stratospheric Chemistry and Transport (1979), Stratospheric ozone depletion by halocarbons: Chemistry and transport, report, pp. 202–218, Natl. Acad. of Sci., Washington, D. C.

Prather, M. J. (1996), Natural modes and time scales in atmospheric chemistry: Theory, GWPs for CH_4 and CO, and runaway growth, *Geophys. Res. Lett.*, *23*, 2597–2600.

Prather, M. J. (1997), Timescales in atmospheric chemistry: CH_3Br, the ocean, and ozone depletion potentials, *Global Biogeochem. Cycles*, *11*(3), 393–400.

Rind, D., D. Shindell, P. Lonergan, and N. K. Balachandrian (1998), Climate change and the middle atmosphere. Part III: The doubled CO_2 climate revisited, *J. Clim.*, *11*, 876–894.

Rind, D., J. Lerner, K. Shah, and R. Suozzo (1999), Use of on-line tracers as a diagnostic tool in general circulation model development: 2. Transport between the troposphere and stratosphere, *J. Geophys. Res.*, *104*, 9151–9167.

Rosenlof, K. H., et al. (2001), Stratospheric water vapor increases over the past half-century, *Geophys. Res. Lett.*, *28*, 1195–1198.

Schmidt, U., and A. Khedim (1991), In situ measurement of carbon dioxide in the winter Arctic vortex and at midlatitudes: An indicator for the 'age' of stratospheric air, *Geophys. Res. Lett.*, *18*, 763–766.

Stratospheric Processes and their Role in Climate (SPARC) (2000), Assessment of upper tropospheric and stratospheric water vapour, edited by D. Kley, J. M. Russell III, and C. Phillips, *Rep. 113*, World Clim. Res. Programme, Geneva, Switzerland.

Wofsy, S. C., and M. B. McElroy (1973), On vertical mixing in the upper stratosphere and lower mesosphere, *J. Geophys. Res.*, *78*, 2619–2624.

Wong, S., M. J. Prather, and D. H. Rind (1999), Seasonal and interannual variability of the budgets of N_2O and CCl_3F, *J. Geophys. Res.*, *104*, 23,899–23,909.

D. H. Ehhalt and F. Rohrer, Forschungszentrum Jülich, Institut II: Troposphäre, Jülich, Germany. (f.rohrer@fz-juelich.de)

M. J. Prather, Department of Earth System Science, University of California, Irvine, Irvine, CA 92697-3100, USA. (mprather@uci.edu)

S. Schauffler, National Center for Atmospheric Research, Boulder, CO 80305, USA. (sues@ucar.edu)